Acta Mech 229, 1703–1719 (2018)
https://doi.org/10.1007/s00707-017-2060-8

ORIGINAL PAPER

Jiakun Zhu · Jun Luo

Effects of entanglements and finite extensibility of polymer chains on the mechanical behavior of hydrogels

Received: 24 July 2017 / Revised: 22 September 2017 / Published online: 23 December 2017

Abstract Polymer networks usually have many entanglements as well as a finite extensibility due to the uncrossability and the full stretching of the network chains. In this paper, the nonaffine model proposed by Davidson and Goulbourne is adopted to characterize the influence of entanglements and finite extensibility of the polymer chains on the mechanical behavior of hydrogels. The Davidson–Goulbourne model only contains three material parameters and has a simpler mathematical form than the Edwards–Vilgis slip-link model, which is the only model that has been adopted to characterize the influence of entanglements on the swelling deformation of polymeric gels so far. Some benchmark problems such as free swelling, constrained swelling, uniaxial tension, equibiaxial tension in the immersed state and uniaxial compression in the isolated state are analyzed, respectively, based on the new constitutive equations. The results show that entanglements as well as chain extensibility have important influences on the mechanical response of hydrogels.

1 Introduction

As a series of polymer materials, hydrogels can absorb a large quantity (even over 90%) of water without dissolving because of the physical or chemical bonds. Hydrogels are ubiquitous and can be found in foods, trees, human and animal bodies, and so on. Their superior biocompatibility and capabilities to imbibe solvents and swell reversibly in response to different stimuli (e.g., temperature, forces, PH values) make them attractive material choices in myriad applications, such as drug-delivery systems [1,2], medical devices [3], tissue engineering [4] and actuators responsive to physiological cues [5].

With the applications in various areas seeing more and more potential, it is imperative to develop constitutive equations to characterize the swelling and deformation behavior of hydrogels. In essence, two approaches have been adopted in the literature to explore the deformation of hydrogels [6]. The first is the multiphasic theory. In this respect, one famous theory is the THB theory, which is the abbreviation of Tanaka et al. [7]. According to the THB theory, the gel is regarded as a biphase combination of a solid and a liquid. Many investigators have used or improved this theory to study the mechanics of hydrogels [6–8]. In spite of its remarkable success, it is well known that the THB theory has certain limitations since it is a linear theory aiming to small swelling ratios. However, it's well known that large deformations are common for hydrogels [9]. What's more, the basic principles of the THB theory are unclear, making it hard to be extended. The second approach, the

J. Zhu · J. Luo (✉)
Department of Mechanics, Huazhong University of Science and Technology, Wuhan, Hubei Province, People's Republic of China
E-mail: jluo@hust.edu.cn; luojun.l@gmail.com
Tel.: 86-27-87543238
Fax: 86-27-87543138

J. Zhu · J. Luo
Hubei Key Laboratory for Engineering Structural Analysis and Safety Assessment, 1037 Luoyu Road, Wuhan 430074, People's Republic of China

monophasic theory, goes back to Biot [10] who established a consolidation theory in terms of fluid-filled elastic porous solids based on thermodynamic theory put forward by Gibbs [11] and Darcy's law. Especially to be mentioned, phenomena including consolidation of soils and deformation of tissues can be studied by Gibbs' and Biot's theories [10,11], which, however, were not specific for hydrogels. Later, some specific models with regard to the free energy of hydrogels have been proposed based on the theories of Gibbs and Biot. The explicit form of the free energy for the hydrogel by combining the Neo-Hookean model of hyperelasticity with the Flory–Huggins mixing model [12,13] goes back to the seminal paper by Flory and Rehner (F–R model) [14]. Hong et al. [15] formulated the nonlinear large deformation constitutive equations for hydrogels based on the F–R model, which have been widely adopted to study the chemo-mechanical coupling behavior of hydrogels [16–18]. It is worth mentioning that the Neo-Hookean model used in the F–R model is the simplest elastic model for elastomers and is derived from the affine assumptions [19]. There has been a surge of the free energy function of rubber hyperelasticity in other forms to characterize the mechanical behavior of hydrogels. To name a few, Dolbow et al. modified the Neo-Hookean model to study chemically induced swelling of hydrogels [20]. On the basis of the Mooney–Rivlin model and the Flory–Huggins mixing theory, Wineman and Rajagopal put forward a particular free energy function for polymer gels [21] which was also chosen by Deng and Pence to investigate the mechanical reactions of polymer gels in both saturated and unsaturated contexts [22,23]. Pieper et al. described swelling in unfilled and filler-loaded networks by means of the van der Waals model [24]. Chester and Anand [25] proposed a free energy function by combining the eight-chain model and Flory–Huggins model to take chain extensibility into account for large deformation behavior of hydrogels. Drozdov and Christiansen [26] derived a constrained chain model to study how the strain rate affects the elastic response of hydrogels in the context of tension and compression. Li et al. [27] adopted the Gent model to study the effect of solvent diffusion on reactive chromotropic polyelectrolyte gel. Very recently, Okumura et al. [28] developed an extended model by introducing two scaling exponents in the elastic strain function and investigated how the scaling exponents influence the swelling behavior of elastomers.

Though the models mentioned above are partially successful in some ways, they are either phenomenological models which ignore the relationship between the microscale behavior of polymer chains and macroscopic properties of elastomers, or physics-based models that do not consider the effect of entanglements and chain extensibility simultaneously. Real polymer networks usually give rise to many entanglements as well as a finite extensibility due to the impenetrability and the full stretching of the network chains, respectively. The effects of entanglements and limited extensibility have been considered in the design of responsive hydrogels [29]. A number of hyperelasticity models have been developed to characterize the influence of entanglements and chain extensibility simultaneously on the mechanical behavior of elastomers. To mention a few, see references [30–35]. However, the corresponding works on hydrogels are rarely found in the open literature. Recently, Yan et al. [36,37] adopted the Edwards–Vilgis slip-link model [34] to predict the effect of chain entanglements on mechanical behavior of polymeric gels. Yang et al. [38] further considered the influence of functionality of junctions in hydrogels. Though the slip-link model can capture the effect of entanglements and chain extensibility, Yan et al. [36,37] and Yang et al. [38] focused more on the influence of entanglements. It should also be pointed out that the slip-link model contains four parameters and its mathematical form is very complicated for theoretical analysis.

Very recently, Davidson and Goulbourne [35] developed a new physics-based nonaffine network model for the nonlinear elasticity of elastomers, which has combined the concepts of the Rubinstein–Panyukov model [39] and Arruda–Boyce model [40]. The Davidson–Goulbourne nonaffine model only contains three material parameters, each of which has clear physical meanings, and has a simpler mathematical form than the slip-link model. The nonaffine model can capture the strain softening, strain hardening, and deformation state-dependent response of rubber materials undergoing finite deformations. This model is unique in its ability to capture large-stretch mechanical behavior with parameters that are connected to the polymer chemistry and can also be easily identified with the important characteristics of the macroscopic stress–stretch response. The contribution of polymer chain entanglements in the nonaffine network model has been confirmed by Li et al. [41] through large-scale MD molecular simulations.

In this paper, a new hybrid energy function is proposed by combining the Davidson–Goulbourne model with the Flory–Huggins solution theory. Constitutive equations are then formulated for the chemo-mechanical equilibrium deformation behaviors of hydrogels. Parameter selection in the new constitutive model is also discussed. After that, several benchmark problems such as free swelling, constrained swelling, uniaxial tension, equibiaxial tension in the immersed state and uniaxial compression in the isolated state are analyzed, respectively, based on the new constitutive equations. The results are compared with those presented by Hong

et al. [42] and those reported by Yan et al. [36]. The influence of entanglements as well as finite extensibility on the mechanical response of hydrogels are fully discussed.

2 Formulation of the constitutive equations

We apply the method proposed by Hong et al. [15] to develop the constitutive equations. According to the Flory theory [14], the free energy of a hydrogel takes the form

$$W(\mathbf{F}, C) = W_S(\mathbf{F}) + W_m(C), \tag{1}$$

where W_s is the free energy due to the stretching of the network and W_m is the free energy due to the mixing of the polymers and solvent. C is the nominal concentration of water molecules. $\mathbf{F}$ is the deformation gradient relative to the dry network. $\mathbf{B} = \mathbf{F}\mathbf{F}^{\mathbf{T}}$ and $\mathbf{C} = \mathbf{F}^{\mathbf{T}}\mathbf{F}$ are the left and right Cauchy–Green deformation tensors, respectively. Principal stretches are defined as the square roots of the eigenvalues of $\mathbf{C}$ (equal to those of $\mathbf{B}$) and are classically denoted λ_i $(i = 1, 2, 3)$.

2.1 Elastic free energy calculated with the nonaffine model

The free energy associated with stretching the network derived from the nonaffine network model [35] can be written as

$$W_s(\mathbf{F}) = \frac{1}{6} G_c \sum_i \lambda_i^2 - G_c \lambda_{\max}^2 \ln\left(3\lambda_{\max}^2 - \sum_i \lambda_i^2\right) + G_e \sum_i \left(\lambda_i + \frac{1}{\lambda_i}\right) - G_c \ln \lambda_1 \lambda_2 \lambda_3, \tag{2}$$

where the last term in Eq. (2) is the volume expansion energy of the matrix [43] and similar terms were introduced in the strain energy density for hydrogels in references [25–27]. λ_i $(i = 1, 2, 3)$ are the principal stretches; k is the Boltzmann constant; T is the absolute temperature; G_c, G_e, $\lambda_{\max}$ are the material parameters accounting for the cross-link density, entanglements and finite extensibility, respectively.

According to Davidson and Goulbourne [35], G_c is defined as the cross-linking modulus and we have $G_c = \frac{kT\rho_m}{N} g^2(1 - 2/\phi)$, where ρ_m is the monomer density;N is the number of monomers in a chain segment; g denotes the affinity of the polymer chain length during deformation and is considered to be a constant. For phantom deformation of polymer chains, we have $g = 1$ and for affine deformation, we have $g = (1-2/\phi)^{-1/2}$. The value of the g may therefore be used to interpolate between phantom and affine network behavior in the range $1 \le g \le (1-2/\phi)^{-1/2}$; ϕ is the cross-link functionality (the number of chains connected at a cross-link) [35]. It is noted that the influence of functionality of junctions in hydrogels was considered by Yang et al. [38]. In this paper, we are not going to discuss the influences of the functionality of junctions. To compare with the result presented by Hong et al. [42], we assume $g = (1-2/\phi)^{-1/2}$. Thus, we have $G_c = kT\rho_m/N = N_R kT$.$N_R$ is the density of cross-links (the number of polymer chains per unit reference volume); k is the Boltzmann constant; T is the absolute temperature. It is noted that in the work by Hong et al. [41], $N_R kT = 10^5$ Pa. In this work, without loss of generality, we set $G_c = 10^5$ Pa.

G_e is the entanglement modulus on behalf of the degree of entanglements in the network. It is noted the coefficient G_e was introduced by Gaylord and Douglas in their localization model [44–47]. In the nonaffine model, we have $G_e = kT\rho_m/N_e$, where N_e is the entanglement length, representing the number of monomers between two adjacent entanglements. In terms of the calculations by Davidson and Goulbourne [35] and Li et al. [41], G_e/G_c varies over a large range depending on the molecular structure of the networks. For larger values of G_e, the chains are more highly entangled with each other. There are basically no entanglements in the network if $G_e = 0$. In our paper we let $G_e = 0, 10G_c, 15G_c, 20G_c$, respectively, to consider different degrees of entanglements.

$\lambda_{\max}$ determines the onset of strain hardening of the network and characterizes the degree of limited extensibility of chains. According to the previous works [35,41], we assume $\lambda_{\max}$ varies from 2 to a very large value.

2.2 Free energy of mixing

The free energy of mixing is most commonly associated with the Flory–Huggins model [12,13], given by the form:

$$W_m(C) = \frac{kT}{v}\left[vC\ln\left(\frac{vC}{1+vC}\right) + \chi\frac{vC}{1+vC}\right], \tag{3}$$

where C is the concentration of solvent molecules in the reference state, v is the volume per small molecule, and χ is a dimensionless Flory interaction parameter. In the isothermal analysis for good solvent, χ is usually taken to be a constant in the range of 0–1.2. In this study, we will take $\chi = 0.1$. It should be mentioned that there are some ways to further improve Eq. (3) [48,49].

2.3 Molecular incompressibility constraint

According to Hong et al. [15], the polymer network and the solvent as well are presumed to be incompressible. The volume of the hydrogel contains that of the dry network along with that of the water. In other words, the change in the volumes of molecules can be neglected because the stress is usually inadequate to lead to molecular distortion. Under this assumption, the constraint is most commonly expressed as:

$$1 + vC = \det \mathbf{F}. \tag{4}$$

Such a constraint is lifted in the studies of Chester et al. [50] and Bouklas et al. [51] to allow a small amount of compressibility, which is substantially aiding in the numerical implementation [50,51]. The relaxation of complete mechanical incompressible on other hypotheses was also proposed by Cai and Suo [52].

2.4 The new total hybrid free energy function

The total hybrid free energy function can be obtained by inserting Eqs. (2) and (3) into Eq. (1):

$$\begin{aligned} W(\mathbf{F}, C) = {} & \frac{1}{6}G_c\sum_i \lambda_i^2 - G_c\lambda_{\max}^2 \ln\left(3\lambda_{\max}^2 - \sum_i \lambda_i^2\right) + G_e\sum_i\left(\lambda_i + \frac{1}{\lambda_i}\right) - G_c\ln\lambda_1\lambda_2\lambda_3 \\ & + \frac{kT}{v}\left[vC\ln\left(\frac{vC}{1+vC}\right) + \chi\frac{vC}{1+vC}\right]. \end{aligned} \tag{5}$$

Subject to the constraint (4), the concentration C in Eq. (5) is no long an independent variable and can be expressed in terms of the deformation gradient $\mathbf{F}$. The enforcement of this constrains are usually carried out in two ways: by using the Lagrange multiplier or Legendre transformation. In practice, we usually know about some information about of the chemical potential but not the nominal concentration C. So we introduce another free energy function W with $\mathbf{F}$ and μ as independent parameters via Legendre transform:

$$C = -\frac{\partial \hat{W}(\mathbf{F}, \mu)}{\partial \mu}, \tag{6}$$

$$\hat{W}(\mathbf{F}, \mu) = W(\mathbf{F}, C) - \mu C. \tag{7}$$

Once the deformation gradient and chemical potential have been solved, the concentration C can be calculated with Eq. (6). Combining Eqs. (4), (5), (6) and (7), we can get:

$$\begin{aligned} \hat{W}(\mathbf{F},\mu) = {} & \frac{1}{6}G_c\sum_i \lambda_i^2 - G_c\lambda_{\max}^2 \ln\left(3\lambda_{\max}^2 - \sum_i \lambda_i^2\right) + G_e\sum_i\left(\lambda_i + \frac{1}{\lambda_i}\right) \\ & - G_c\ln J + \frac{kT}{v}\left[(J-1)\ln\frac{J-1}{J} + \chi\frac{J-1}{J}\right] - \frac{\mu}{v}(J-1). \end{aligned} \tag{8}$$

2.5 Specific constitutive equations

In this study, we are concerned with the equilibrium state of the hydrogel rather than the instantaneous migration process of the water molecules. For large deformation problems, the nominal (or the first Piola–Kirchhoff) stress tensors can be obtained by:

$$\mathbf{P} = \frac{\partial \hat{W}}{\partial \mathbf{F}}. \tag{9}$$

The true (or Cauchy) stress tensor $\boldsymbol{\sigma}$ and $\mathbf{P}$ are related by:

$$\boldsymbol{\sigma} = (\det \mathbf{F})^{-1}\mathbf{P}\mathbf{F}^T = \frac{1}{J}\mathbf{P}\mathbf{F}^T = \frac{1}{J}\frac{\partial \hat{W}}{\partial \mathbf{F}}\mathbf{F}^T. \tag{10}$$

Substitution of Eq. (8) into Eq. (10), we get the Cauchy stress tensor:

$$\boldsymbol{\sigma} = \frac{2}{J}\mathbf{F}\frac{\partial W_s}{\partial \mathbf{C}}\mathbf{F}^T + \left(\frac{kT}{v}\left[\frac{1}{J} - \ln\left(\frac{J}{J-1}\right) + \frac{\chi}{J^2}\right] - \frac{\mu}{v}\right)\mathbf{I}. \tag{11}$$

Referring to Eq. (9), the principal nominal stresses P_i can be expressed as functions of three principal stretches, λ_i $(i = 1, 2, 3)$:

$$\begin{aligned}\frac{p_1 v}{kT} &= \frac{\lambda_1}{3}\frac{G_c v}{kT} + \frac{G_c v}{kT}\lambda_{\max}^2\frac{2\lambda_1}{(3\lambda_{\max}^2 - \lambda_1^2 - \lambda_2^2 - \lambda_3^2)} + \frac{G_e v}{kT}\left(1 - \frac{1}{\lambda_1^2}\right)\\ &\quad + \lambda_2\lambda_3\left[\ln\left(1 - \frac{1}{\lambda_1\lambda_2\lambda_3}\right) + \frac{1}{\lambda_1\lambda_2\lambda_3} + \frac{\chi}{(\lambda_1\lambda_2\lambda_3)^2}\right] - \frac{G_c v}{kT\lambda_1} - \frac{\mu}{kT}\lambda_2\lambda_3, \qquad (12)\\ \frac{p_2 v}{kT} &= \frac{\lambda_2}{3}\frac{G_c v}{kT} + \frac{G_c v}{kT}\lambda_{\max}^2\frac{2\lambda_2}{(3\lambda_{\max}^2 - \lambda_1^2 - \lambda_2^2 - \lambda_3^2)} + \frac{G_e v}{kT}\left(1 - \frac{1}{\lambda_2^2}\right)\\ &\quad + \lambda_1\lambda_3\left[\ln\left(1 - \frac{1}{\lambda_1\lambda_2\lambda_3}\right) + \frac{1}{\lambda_1\lambda_2\lambda_3} + \frac{\chi}{(\lambda_1\lambda_2\lambda_3)^2}\right] - \frac{G_c v}{kT\lambda_2} - \frac{\mu}{kT}\lambda_1\lambda_3, \qquad (13)\\ \frac{p_3 v}{kT} &= \frac{\lambda_3}{3}\frac{G_c v}{kT} + \frac{G_c v}{kT}\lambda_{\max}^2\frac{2\lambda_3}{(3\lambda_{\max}^2 - \lambda_1^2 - \lambda_2^2 - \lambda_3^2)} + \frac{G_e v}{kT}\left(1 - \frac{1}{\lambda_3^2}\right)\\ &\quad + \lambda_2\lambda_1\left[\ln\left(1 - \frac{1}{\lambda_1\lambda_2\lambda_3}\right) + \frac{1}{\lambda_1\lambda_2\lambda_3} + \frac{\chi}{(\lambda_1\lambda_2\lambda_3)^2}\right] - \frac{G_c v}{kT\lambda_3} - \frac{\mu}{kT}\lambda_2\lambda_1. \qquad (14)\end{aligned}$$

Equations (12)–(14) are the constitutive equations at the equilibrium state. We have normalized the stress by kT/v, and normalized the chemical potential by kT.

3 Analytical results

In this section, several benchmark problems of homogeneous deformations of hydrogel are analyzed by utilizing the developed constitutive equations. The effects of the microstructural parameters G_e and $\lambda_{\max}$, which describe the entanglements and finite extensibility of the network, respectively, on the mechanical response of the hydrogel are fully discussed. Some of these problems have been analyzed by Hong et al. [42] and Yan et al. [36] by using the Neo-Hookean model of elasticity and the slip-link model of elasticity, respectively. Our results are compared with those presented by Hong et al. [42] and those reported by Yan et al. [36].

3.1 Free swelling

In the absence of the mechanical load and immersed in a reservoir of solvent molecules, the hydrogel swells with no restriction till the solvent chemical potential reaches a balance with the reservoir. In this state, the

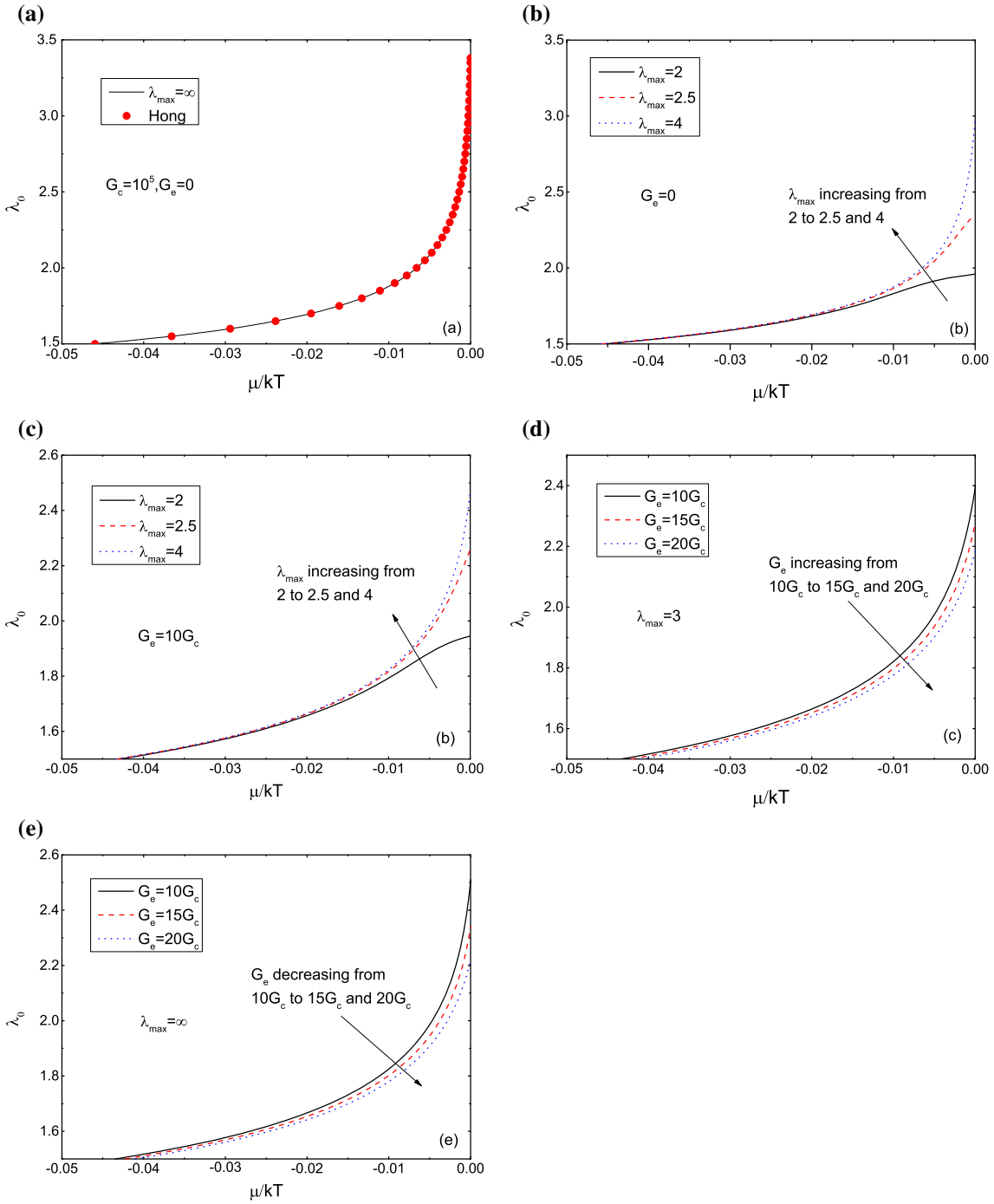

Fig. 1 Variation of the free swelling ratio of a cubic hydrogel with the chemical potential of the solvent molecules. **a** $G_e = 0$, $\lambda_{\max} = \infty$; **b** $G_e = 0$. $\lambda_{\max}$ takes different values; **c** $G_e = 10G_c$. $\lambda_{\max}$ takes different values; **d** $\lambda_{\max} = 3$. G_e takes different values; **e** $\lambda_{\max} = \infty$. G_e takes different values

hydrogel swells to the same degree in all directions. We denote this free swelling ratio by $\lambda_1 = \lambda_2 = \lambda_3 = \lambda_0$, setting the stresses in Eqs. (12)–(14) to be zero, we obtain:

$$\frac{vG_c}{3\lambda_0 kT} + \frac{vG_c}{kT}\lambda_{\max}^2 \frac{2}{\lambda_0(3\lambda_{\max}^2 - 3\lambda_0^2)} + \frac{vG_e}{kT}\left(\frac{1}{\lambda_0^2} - \frac{1}{\lambda_0^4}\right) + \left[\ln\left(1 - \frac{1}{\lambda_0^3}\right) + \frac{1}{\lambda_0^3} + \frac{\chi}{\lambda_0^6}\right] - \frac{G_c v}{kT\lambda_0^3} = \frac{\mu}{kT}. \tag{15}$$

This relation determines the free swelling stretch λ_0 once the chemical potential is known. λ_0 is plotted against the normalized chemical potential μ/kT in Fig. 1 for different material parameters, i.e., G_e and $\lambda_{\max}$. The results of Hong et al. [42] are also plotted in Fig. 1a for a comparison. It can be readily observed that if we don't consider the effect of the entanglements and limited extensibility of the polymer chains, our results can reduce to those given by Hong et al. [42]. It should be mentioned that as the maximum free swelling ratio of the hydrogel is about 3.4 in Fig. 1a, $\lambda_{\max}$ is set to a very large value (e.g., $\lambda_{\max} = 10{,}000$) in the numerical computation in Fig. 1a to exclude the influence of finite extensibility. In the other studies, we use the same method to exclude the influence of the limited extensibility of the polymer chains.

As illustrated in Fig. 1b, c, the free swelling ratio increases with $\lambda_{\max}$. This is natural since a larger value of $\lambda_{\max}$ implies that the free swelling of the hydrogel is less constrained by the finite extensibility of the polymer chains. This conclusion is similar with that drawn by Yan et al. [36] (the free swelling ratio of the gel with larger value of α is lower where α is the inextensibility parameter in the slip-link model). Chester and Anand came to the same conclusion by using the eight-chain model [25]. Another interesting finding from Fig. 1b, c is that the ultimate free swelling ration is no more than $\lambda_{\max}$.

Referring to Fig. 1d, e, we can also find that when G_e is larger (corresponding to more dense entanglements), the final free swelling ratio is lower. This is reasonable from our intuition and has been confirmed by Chen et al. by using Monte Carlo simulations [53]. However, it is noted that the free swelling ratio increases with the density of entanglements, i.e., $N_s/(N_c + N_s)$ in the work by Yan et al. [36].

3.2 Biaxial constrained swelling

In this section, we consider the swelling of a thin layer of hydrogel bonded on a rigid substrate. Since the thickness of the layer is thin, one can assume that the hydrogel experiences biaxial constrained swelling. Following Hong et al. [42] and Yan et al. [36], we assume that the prestretches of the hydrogel to be $\lambda_2 = \lambda_3 = \lambda_0 = 1.5$. Subsequently, the hydrogel is immersed in pure water with the chemical potential $\mu = 0$. Due to the constraint of the substrate, the gel layer swells to a further stretch λ_1 along the normal direction of the blanket gel layer and achieves another equilibrium state with an equal-biaxial stress. The stress normal to the blanket layer vanishes, so that Eq. (12) gives:

$$\begin{aligned}&\frac{\lambda_1}{3\lambda_0^2}\frac{G_c v}{kT} + \frac{G_c v}{kT}\lambda_{\max}^2 \frac{2\lambda_1}{\lambda_0^2\left(3\lambda_{\max}^2 - \lambda_1^2 - 2\lambda_0^2\right)} + \frac{G_e v}{kT}\left(\frac{1}{\lambda_0^2} - \frac{1}{\lambda_1^2\lambda_0^2}\right)\\ &+\left[\ln\left(1 - \frac{1}{\lambda_1\lambda_0^2}\right) + \frac{1}{\lambda_1\lambda_0^2} + \frac{\chi}{\left(\lambda_1\lambda_0^2\right)^2}\right] - \frac{G_c v}{kT\lambda_1\lambda_0^2} = \frac{\mu}{kT},\end{aligned} \tag{16}$$

where the two in-plane stretches hold to be the initial value due to confinement by the rigid substrate, but the out-of-plane stretch varies with the chemical potential. The normalized in-plane biaxial stress can be expressed as:

$$\begin{aligned}\frac{p_2 v}{kT} &= \frac{\lambda_0}{3}\frac{G_c v}{kT} + \frac{G_c v}{kT}\lambda_{\max}^2 \frac{2\lambda_0}{\left(3\lambda_{\max}^2 - \lambda_1^2 - 2\lambda_0^2\right)} + \frac{G_e v}{kT}\left(1 - \frac{1}{\lambda_0^2}\right) + \lambda_1\lambda_0\\ &+\left[\ln\left(1 - \frac{1}{\lambda_1\lambda_0^2}\right) + \frac{1}{\lambda_1\lambda_0^2} + \frac{\chi}{\left(\lambda_1\lambda_0^2\right)^2}\right] - \frac{G_c v}{kT\lambda_0} - \frac{\mu}{kT}\lambda_1\lambda_0.\end{aligned} \tag{17}$$

Referring to Eq. (16), we plot the stretch λ normal to the blanket layer against the chemical potential μ/kT for different values of G_e and $\lambda_{\max}$, as shown in Fig. 2. In the absence of entanglements and limited extensibility, our results can reduce to the those obtained by Hong et al. [42]. Similar to the free swelling, higher entanglement modulus and lower extensibility cause the blanket gel layer to swell less, i.e., when the network is more densely entangled and the limited extensibility is less, the stretch of the hydrogel in the direction normal to the layer is smaller. This conclusion is consistent with Yan et al.'s result [36]. It is of interest to see that the stretch perpendicular to the layer direction can be significantly increased to even more than $\lambda_{\max}$ by the biaxial constraint. However, in the case of free swelling, the swelling ratio is always less than $\lambda_{\max}$ as shown in Fig. 1.

According to Eq. (17), variation of the normalized equal-biaxial compressive stress is plotted against the chemical potential for different values of G_e and $\lambda_{\max}$in Fig. 3. It can be easily observed that the magnitude of

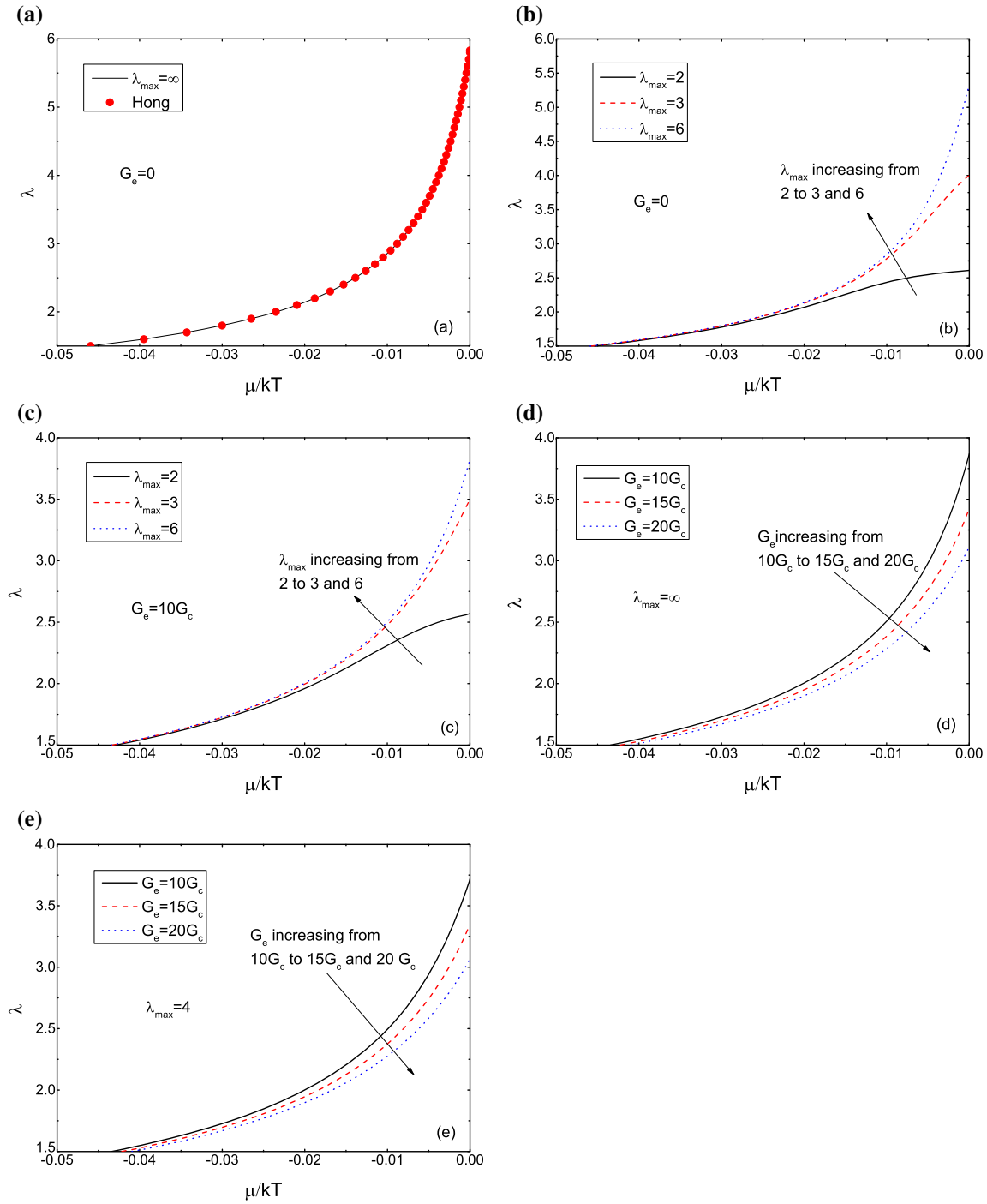

Fig. 2 Variation of the biaxial constrained swelling ratio of a hydrogel layer with the chemical potential of the solvent molecules. **a** $G_e = 0$, $\lambda_{\max} = \infty$; **b** $G_e = 0$. $\lambda_{\max}$ takes different values; **c** $G_e = 10G_c$. $\lambda_{\max}$ takes different values; **d** $\lambda_{\max} = \infty$. G_e takes different values; **e** $\lambda_{\max} = 4$. G_e takes different values

the equal-biaxial compressive stress increases with the increase in G_e and the decrease in $\lambda_{\max}$, this conclusion is also consistent with Yan et al.'s result [36]. Moreover, comparing Fig. 3b with 3c, the discrepancies brought by the differences of chain extensibility will be weakened by the entanglements.

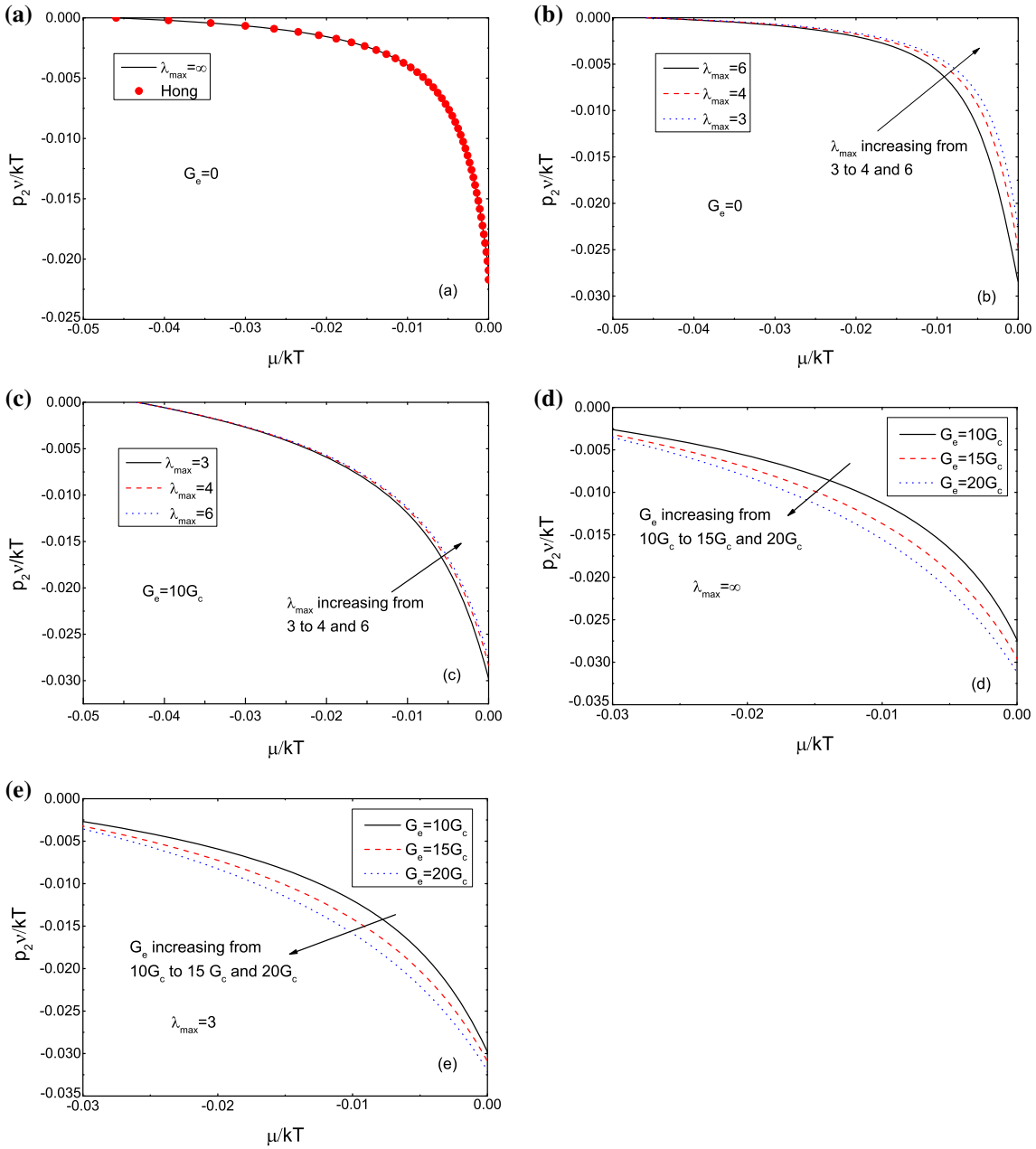

Fig. 3 Variation of the equibiaxial compressive stress with the chemical potential of the solvent molecules. **a** $G_e = 0$, $\lambda_{\max} = \infty$; **b** $G_e = 0$. $\lambda_{\max}$ takes different values; **c** $G_e = 10G_c$. $\lambda_{\max}$ takes different values; **d** $\lambda_{\max} = \infty$. G_e takes different various; **e** $\lambda_{\max} = 3$. G_e takes different values

3.3 Uniaxial tension

We assume that a bar of a hydrogel is equilibrated in a solvent of chemical potential μ and is subject to a uniaxial stress along the axial direction. The deformation state can be characterized by principal stretches, λ_i $(i = 1, 2, 3)$ where λ_1 is along the axial direction. λ_2 and λ_3 are principle stretches along the transverse directions, and we have $\lambda_2 = \lambda_3$. As the transverse normal stresses are zero, referring to Eqs. (13) and (14), we have:

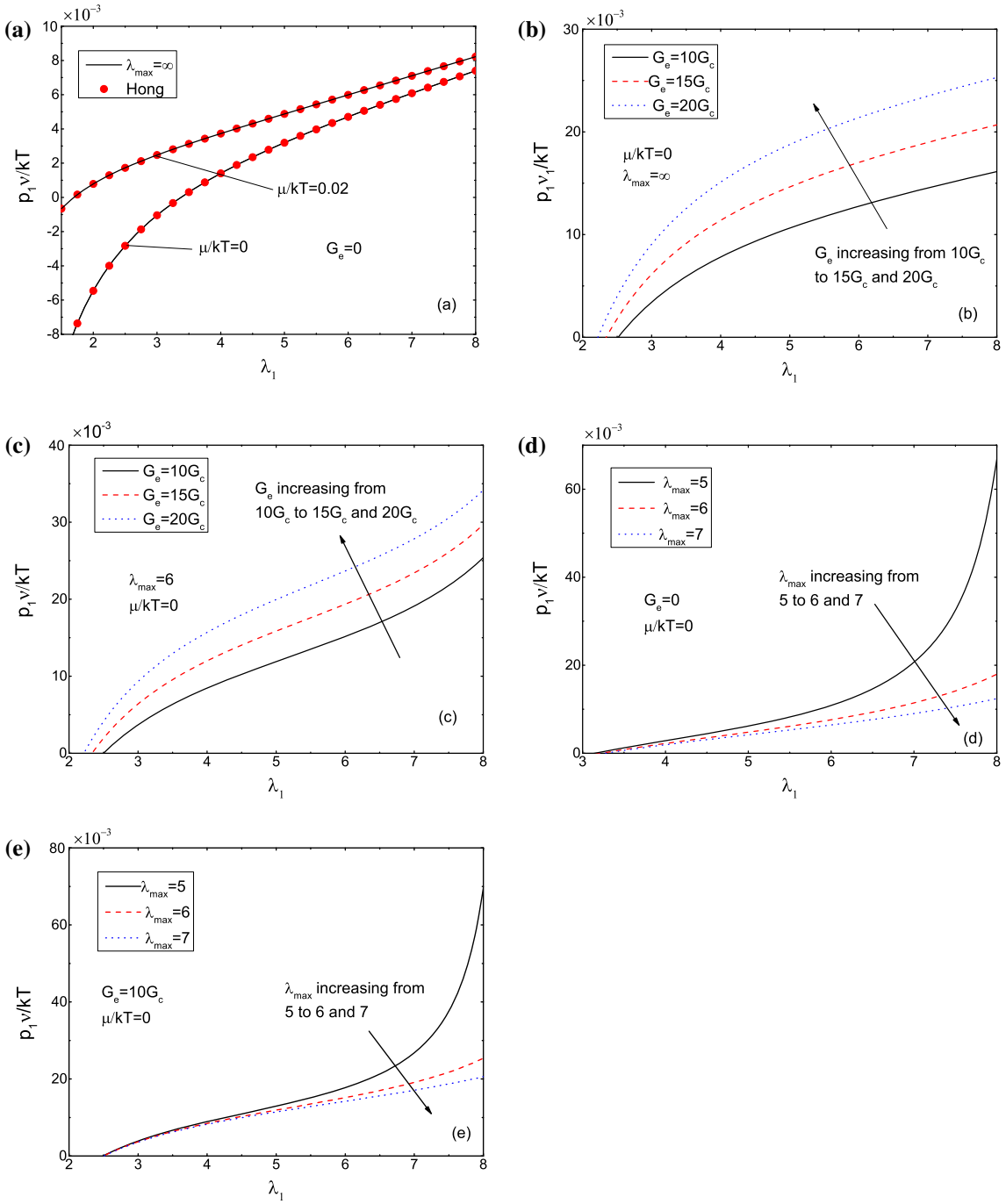

Fig. 4 Variation of the uniaxial stress with the axial stretch. **a** $G_e = 0,\ \lambda_{\max} = \infty, \mu/kT = 0,\ -0.02$; **b** $\lambda_{\max} = \infty$. G_e takes different values; **c** $\lambda_{\max} = 6$. G_e takes different values; **d** $G_e = 0$. $\lambda_{\max}$ takes different values; **e** $G_e = 10G_c$. $\lambda_{\max}$ takes different values

$$\frac{1}{3\lambda_1}\frac{G_c v}{kT} + \frac{G_c v}{kT}{}_c\lambda_{\max}^2 \frac{2}{\lambda_1(3\lambda_{\max}^2 - \lambda_1^2 - 2\lambda_2^2)} + \frac{G_e v}{kT}\left(\frac{1}{\lambda_1\lambda_2} - \frac{1}{\lambda_2^3\lambda_1}\right) + \left[\ln\left(1 - \frac{1}{\lambda_1\lambda_2^2}\right) + \frac{1}{\lambda_1\lambda_2^2} + \frac{\chi}{(\lambda_1\lambda_2^2)^2}\right] - \frac{G_c v}{kT\lambda_1\lambda_2^2} - \frac{\mu}{kT} = 0. \tag{18}$$

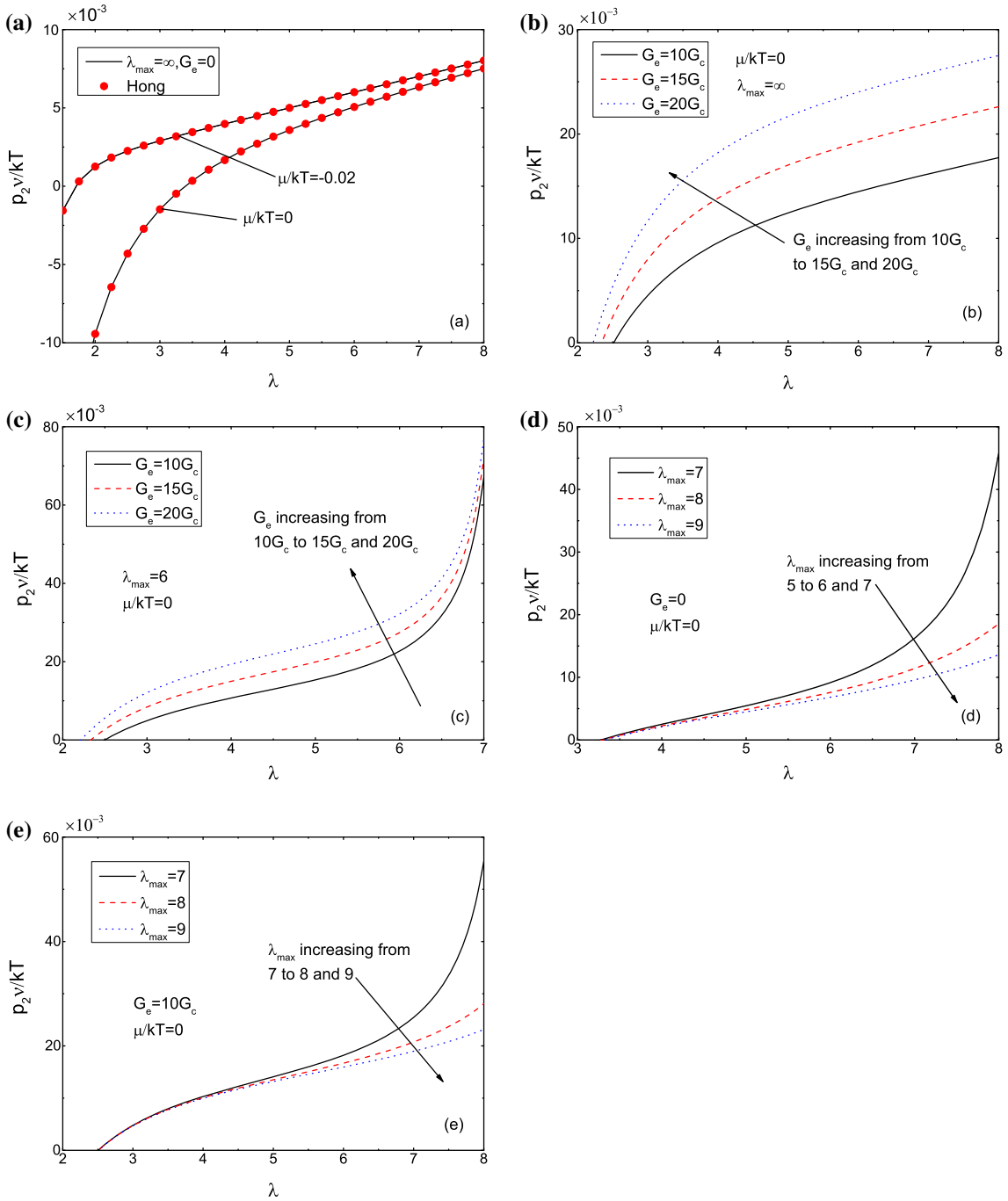

Fig. 5 Variation of the equibiaxial stress with the stretch. **a** $G_e = 0$, $\lambda_{\max} = \infty$, $\mu/kT = 0, \ -0.02$; **b** $\lambda_{\max} = \infty$. G_e takes different values; **c** $\lambda_{\max} = 6$. G_e takes different values; **d** $G_e = 0$. $\lambda_{\max}$ takes different values; **e** $G_e = 10G_c$. $\lambda_{\max}$ takes different values

We can calculate λ_2 with Eq. (18) once λ_1 is given. λ_1 is related with the nominal uniaxial stress by:

$$\frac{p_1 v}{kT} = \frac{\lambda_1}{3}\frac{G_c v}{kT} + \frac{G_c v}{kT}\lambda_{\max}^2 \frac{2\lambda_1}{(3\lambda_{\max}^2 - \lambda_1^2 - 2\lambda_2^2)} + \frac{G_e v}{kT}\left(1 - \frac{1}{\lambda_1^2}\right) + \left[\lambda_2^2 \ln\left(1 - \frac{1}{\lambda_1\lambda_2^2}\right) + \frac{1}{\lambda_1} + \frac{\chi}{\lambda_1^2\lambda_2^2}\right] - \frac{G_c v}{kT\lambda_1} - \lambda_2^2\frac{\mu}{kT}. \tag{19}$$

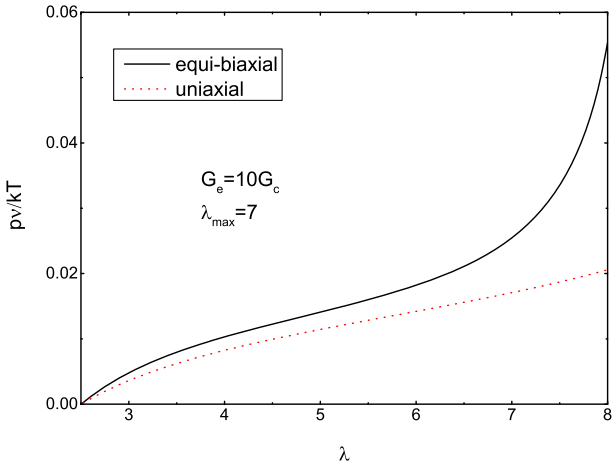

Fig. 6 Comparison of the uniaxial stress and biaxial stress at different stretch ratios

Figure 4a–e show the relation between the nominal uniaxial stress and the axial stretch λ_1. Figure 4a indicates that our results can reduce to those presented by Hong et al. [42] if the effects of entanglements and limited extensibility have been ignored. It's worth to mention that when the uniaxial stress is negative, the hydrogel is under uniaxial constrained swelling, which will not be discussed here. Thus, in Fig. 4b–e, we assume that the hydrogel is in tension after the initial free swelling.

As shown in Fig. 4b, c, we can see that whether the limited extensibility takes effect or not, the nominal stress increases with G_e for a given stretch ratio, or in other words, the stretch ratio λ_1 decreases when G_e increases for a given uniaxial stress. This is reasonable as the hydrogel has become stiffer when there are more entanglements in network. Similar conclusions have been drawn by Yan et al. [36] and Chen et al. [53].

In Fig. 4d, e, we can see that for a given stretch ratio, the nominal uniaxial stress increases when $\lambda_{\max}$ decreases. This is because a smaller value of $\lambda_{\max}$ implies that the strain stiffening takes place earlier and as a result, the stress becomes larger. When the stretch ratio of the hydrogel is greater than $\lambda_{\max}$, the uniaxial stress increases dramatically with the stretch ratio. In this case, the influence of entanglements on the uniaxial stress has become less important, as shown in Fig. 4d, e.

3.4 Equibiaxial tension

Now we consider a cubic block of a hydrogel immersed in a solvent of chemical potential μ, and subject to an equibiaxial tensile stress. Again, the deformation state of the block can be characterized by three principle stretches, λ_i $(i = 1, 2, 3)$. Here, we assume the biaxial tensile stresses are applied along the second and third principal directions. Thus, we have $\lambda_2 = \lambda_3$. As the first principal stress is zero, referring to Eq. (12), we have:

$$\frac{\lambda_1}{3}\frac{G_c v}{kT} + \frac{G_c v}{kT}\lambda_{\max}^2 \frac{2\lambda_1}{(3\lambda_{\max}^2 - \lambda_1^2 - 2\lambda_2^2)} + \frac{G_e v}{kT}\left(1 - \frac{1}{\lambda_1^2}\right) + \lambda_2^2\left[\ln\left(1 - \frac{1}{\lambda_1\lambda_2^2}\right) + \frac{1}{\lambda_1\lambda_2^2} + \frac{\chi}{(\lambda_1\lambda_2^2)^2}\right] - \frac{G_c v}{kT\lambda_1} - \lambda_2^2\frac{\mu}{kT} = 0. \tag{20}$$

The equibiaxial stress is related to the transverse principal stretch, i.e., λ_2 or λ_3 through:

$$\frac{p_2 v}{kT} = \frac{\lambda_2}{3}\frac{G_c v}{kT} + \frac{G_c v}{kT}\lambda_{\max}^2 \frac{2\lambda_2}{(3\lambda_{\max}^2 - \lambda_1^2 - 2\lambda_2^2)} + \frac{G_e v}{kT}\left(1 - \frac{1}{\lambda_2^2}\right) + \lambda_1\lambda_2\left[\ln\left(1 - \frac{1}{\lambda_1\lambda_2^2}\right) + \frac{1}{\lambda_1\lambda_2^2} + \frac{\chi}{(\lambda_1\lambda_2^2)^2}\right] - \frac{G_c v}{kT\lambda_2} - \frac{\mu}{kT}\lambda_1\lambda_2. \tag{21}$$

The equibiaxial stress is plotted against the transverse principle stretch in Fig. 5. Similarly, we only consider the situation that the hydrogel is under tensile stresses. In Fig. 5a, a comparison is made between our results and

those by using the Flory–Rehner free energy function. As shown in Fig. 5a, in the absence of entanglements and finite extensibility, our results match well with those obtained by the Flory–Rehner model [42]. Figure 5b–e shows that the equibiaxial stress increases with the increase in G_e and decrease in $\lambda_{\max}$. Comparing Fig. 5c and Fig. 4c, we can see that when the stretch ratio exceeds $\lambda_{\max}$, the equibiaxial stress increases more dramatically than the uniaxial stress. Furthermore, under the same stretch ratio, we can see from Fig. 6 that the biaxial stress is greater than the uniaxial stress, which is in accordance with the experimental data in the literature [54,55].

3.5 Uniaxial compression

In this section, we discuss the deformation behavior of a swollen cubic hydrogel under uniaxial compression. As demonstrated in Fig. 7, a cubic of a hydrogel is put on a rigid substrate, with stress free preswelling of an isotropic stretch λ_0. Unlike the former cases where the hydrogel is assumed to be immersed in the solvent, in this case, we assume that the hydrogel is isolated from the solvent after free swelling. To study this problem conveniently, we choose the swollen state as the reference state [56]. As proposed by Hong et al. [42], we denote $\mathbf{F}' = \mathrm{diag}(\lambda_1, \lambda_2, \lambda_3)$ and $\hat{W}'(\mathbf{F}', \mu)$ to be the deformation tensor and the free energy functional of the hydrogel, respectively. Then, the deformation tensor is $\mathbf{F} = \mathbf{F}'\mathbf{F}_0$ when we take the dry gel as the reference state. In virtue of $\hat{W}'(\mathbf{F}', \mu)\mathrm{d}V' = \hat{W}(\mathbf{F}, \mu)\,\mathrm{d}V$, $\mathrm{d}V' = \lambda_0^3 \mathrm{d}V$, we get:

$$\hat{W}'(\mathbf{F}', \mu) = \lambda_0^{-3}\hat{W}(\mathbf{F}, \mu). \tag{22}$$

Combining Eqs. (8) and (22), we obtain that

$$\begin{aligned} W'(\mathbf{F}'', \mu) = {} & \frac{\lambda_0^{-1}}{6} G_c \sum_i \lambda_i^2 - \lambda_0^{-3} G_c \lambda_{\max}^2 \ln\left(3\lambda_{\max}^2 - \lambda_0^2 \sum_i \lambda_i^2\right) + G_e \lambda_0^{-2} \sum_i \lambda_i \\ & + G_e \lambda_0^{-4} \sum_i \frac{1}{\lambda_i} - \lambda_0^{-3} G_c \ln\left(\lambda_0^3 J\right) + \frac{kT}{v}\left[(J - \lambda_0^{-3}) \ln \frac{\lambda_0^3 J - 1}{\lambda_0^3 J} - \chi \frac{\lambda_0^3 J - 1}{\lambda_0^6 J}\right] - \frac{\mu}{v}(J - \lambda_0^{-3}). \end{aligned} \tag{23}$$

Substitution of Eq. (23) into Eq. (10) yields

$$\begin{aligned} \frac{\sigma_1 v}{kT} = {} & \frac{\lambda_0^{-1}}{3}\frac{G_c v}{kT}\lambda_1^2 + \lambda_0^{-3}\frac{G_c v}{kT}\lambda_{\max}^2 \frac{2\lambda_0^2\lambda_1^2}{3\lambda_{\max}^2 - \lambda_0^2(\lambda_1^2 + \lambda_2^2 + \lambda_3^2)} + \lambda_0^{-2}\frac{G_e v}{kT}\lambda_1 - \lambda_0^{-4}\frac{G_c v}{kT}\frac{1}{\lambda_1} \\ & + \left[\lambda_1\lambda_2\lambda_3 \ln\left(1 - \frac{1}{\lambda_0^3\lambda_1\lambda_2\lambda_3}\right) + \frac{1}{\lambda_0^3} + \frac{\chi}{\lambda_0^6\lambda_1\lambda_2\lambda_3}\right] - \lambda_0^{-3}\frac{G_c v}{kT} - \frac{\mu}{kT}, \end{aligned} \tag{24}$$

$$\begin{aligned} \frac{\sigma_2 v}{kT} = {} & \frac{\lambda_0^{-1}}{3}\frac{G_c v}{kT}\lambda_2^2 + \lambda_0^{-3}\frac{G_c v}{kT}\lambda_{\max}^2 \frac{2\lambda_0^2\lambda_2^2}{3\lambda_{\max}^2 - \lambda_0^2(\lambda_1^2 + \lambda_2^2 + \lambda_3^2)} + \lambda_0^{-2}\frac{G_e v}{kT}\lambda_2 - \lambda_0^{-4}\frac{G_c v}{kT}\frac{1}{\lambda_2} \\ & + \left[\lambda_1\lambda_2\lambda_3 \ln\left(1 - \frac{1}{\lambda_0^3\lambda_1\lambda_2\lambda_3}\right) + \frac{1}{\lambda_0^3} + \frac{\chi}{\lambda_0^6\lambda_1\lambda_2\lambda_3}\right] - \lambda_0^{-3}\frac{G_c v}{kT} - \frac{\mu}{kT}, \end{aligned} \tag{25}$$

$$\begin{aligned} \frac{\sigma_3 v}{kT} = {} & \frac{\lambda_0^{-1}}{3}\frac{G_c v}{kT}\lambda_3^2 + \lambda_0^{-3}\frac{G_c v}{kT}\lambda_{\max}^2 \frac{2\lambda_0^2\lambda_3^2}{3\lambda_{\max}^2 - \lambda_0^2(\lambda_1^2 + \lambda_2^2 + \lambda_3^2)} + \lambda_0^{-2}\frac{G_e v}{kT}\lambda_3 \\ & - \lambda_0^{-4}\frac{G_c v}{kT}\frac{1}{\lambda_3} + \left[\lambda_1\lambda_2\lambda_3 \ln\left(1 - \frac{1}{\lambda_0^3\lambda_1\lambda_2\lambda_3}\right) + \frac{1}{\lambda_0^3} + \frac{\chi}{\lambda_0^6\lambda_1\lambda_2\lambda_3}\right] - \lambda_0^{-3}\frac{G_c v}{kT} - \frac{\mu}{kT}. \end{aligned} \tag{26}$$

The state of deformation can be characterized by: stretch λ_1 along the direction of the pressure and two transverse stretches $\lambda_2 = \lambda_3$. As the stresses in the directions of λ_2 and λ_3 vanish, we have:

$$\begin{aligned} & \frac{\lambda_0^{-1}}{3}\frac{G_c v}{kT}\lambda_2^2 + \lambda_0^{-3}\frac{G_c v}{kT}\lambda_{\max}^2 \frac{2\lambda_0^2\lambda_2^2}{3\lambda_{\max}^2 - \lambda_0^2(\lambda_1^2 + 2\lambda_2^2)} + \lambda_0^{-2}\frac{G_e v}{kT}\lambda_2 - \lambda_0^{-4}\frac{G_c v}{kT}\frac{1}{\lambda_2} \\ & + \left[\lambda_1\lambda_2^2 \ln\left(1 - \frac{1}{\lambda_0^3\lambda_1\lambda_2^2}\right) + \frac{1}{\lambda_0^3} + \frac{\chi}{\lambda_0^6\lambda_1\lambda_2^2}\right] - \lambda_0^{-3}\frac{G_c v}{kT} - \frac{\mu}{kT} = 0. \end{aligned} \tag{27}$$

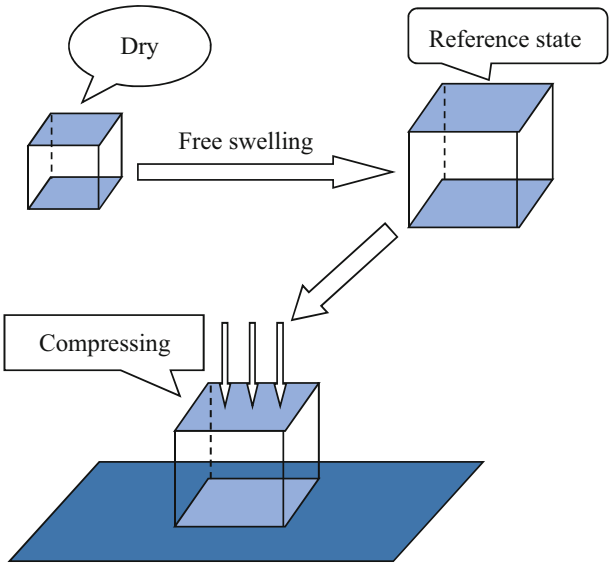

Fig. 7 A swollen hydrogel compressed by uniaxial pressure

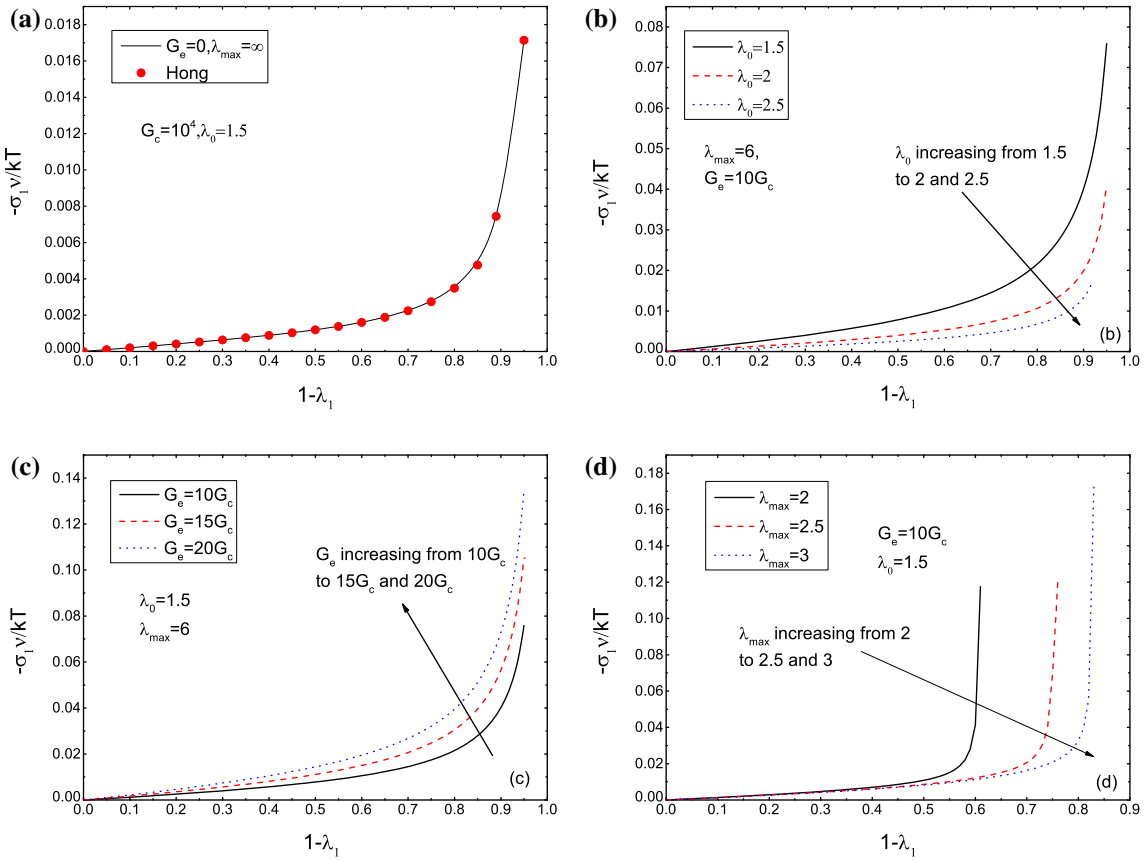

Fig. 8 Strain–stress of uniaxial compression for a swollen hydrogel. **a** $G_e = 0$, $\lambda_{\max} = \infty$, $\lambda_0 = 1.5$; **b** $G_e = 10G_c$, $\lambda_{\max} = 10$. λ_0 takes various values; **c** $\lambda_0 = 1.5$, $\lambda_{\max} = 10$.G_e takes various values; **d** $G_e = 10G_c$, $\lambda_0 = 1.5$. $\lambda_{\max}$ takes various values

We assume there is no solvent loss in the compression process. Thus, the volume of the hydrogel is conserved during the deformation, and we have [56]

$$\det \mathbf{F} = \lambda_1\lambda_2\lambda_3 = \lambda_1\lambda_2^2 = 1. \tag{28}$$

Combination of Eqs. (24), (27) and Eq. (28) yields

$$\begin{aligned}\frac{\sigma_1 v}{kT} = {} & \frac{\lambda_0^{-1}}{3}\frac{G_c v}{kT}\left(\lambda_1^2 - \frac{1}{\lambda_1}\right) + \lambda_0^{-1}\frac{G_c v}{kT}\lambda_{\max}^2\frac{2(\lambda_1^3-1)}{3\lambda_{\max}^2\lambda_1 - \lambda_0^2(\lambda_1^3+2)} \\ & + \lambda_0^{-2}\frac{G_e v}{kT}\left(\lambda_1 - \sqrt{\frac{1}{\lambda_1}}\right) + \lambda_0^{-4}\frac{G_e v}{kT}\left(\sqrt{\lambda_1} - \frac{1}{\lambda_1}\right).\end{aligned} \tag{29}$$

Equation (29) shows the relation between the compression deformation and compression stress, which is plotted in Fig. 8. In Fig. 8, the minus in the front of $\sigma v/kT$ means that the direction of the stress is reversed. Figure 8a shows that our results can be reduced to those obtained by the Flory–Rehner model. In Fig. 8b, we can see that when the free swelling ratio is higher, smaller stresses are needed to compress the hydrogel to the same compression deformation, i.e., $1-\lambda_1$. This is reasonable as the hydrogel has become softer when more water has been absorbed into the hydrogel (larger free swelling ratio). From Fig. 8c, we can see that when G_e is greater, the compression stress is higher. This seems natural since the hydrogel has become stiffer when there are more entanglements in the network.

Figure 8d is very interesting, and we may be confused at first glance. In the beginning, $\lambda_{\max}$ has no influence on stress, but in the later process, the small $\lambda_{\max}$ is, the higher stress is, and the upward trend of the stress becomes very sharp and abrupt. This means that in the case of the volume of the hydrogel is an invariant, with the compress of it, the hydrogel in other two directions will expand; and when the rate of expansion surpass $\lambda_{\max}$, the stress used to compress will increases in a sharp speed.

4 Concluding remarks

In this paper, a new hybrid free energy function composed of the nonaffine model and the Flory–Huggins solution theory is proposed to investigate the influences of chain entanglements and limited chain extensibility on the mechanical response of hydrogels. The nonaffine model contains fewer material parameters and has a simpler mathematical form than the Edwards–Vilgis slip-link model. This new hybrid free energy function can be reduced to the Flory–Rehner function if the influences of the entanglements and chain extensibility are ignored. The nonlinear large deformation constitutive equations of the hydrogel are derived based on the new free energy function. Five benchmark problems are analyzed by using the new constitutive equations. The numerical results show that entanglements and limited chain extensibility have distinct influences on the mechanical responses of hydrogels.

Acknowledgements This work is supported by the National Natural Science Foundation of China (Grant No. 11372114).

References

1. Peppas, N.A., Bures, P., Leobandung, W., Ichikawa, H.: Hydrogels in pharmaceutical formulations. Eur. J. Pharm. Biopharm. **50**, 27–46 (2000)
2. Qiu, Y., Park, K.: Environment-sensitive hydrogels for drug delivery. Adv. Drug. Deliv. Rev. **53**, 321–339 (2001)
3. Peppas, N.A., Hilt, J.Z., Khademhosseini, A., Langer, R.: Hydrogels in biology and medicine: from molecular principles to bionanotechnology. Adv. Mater. **18**, 1345–1360 (2006)
4. Nguyen, K.T., West, J.L.: Photopolymerizable hydrogels for tissue engineering applications. Biomaterials **23**, 4307–4314 (2002)
5. Cho, E.C., Kim, J.W., Fernandez-Nieves, A., Weitz, D.A.: Highly responsive hydrogel scaffolds formed by three-dimensional organization of microgel nanoparticles. Nano Lett. **8**, 168–172 (2008)
6. Hui, C.Y., Muralidharan, V.: Gel mechanics: a comparison of the theories of Biot and Tanaka, Hocker, and Benedek. J. Chem. Phys. **123**, 154905 (2005)
7. Tanaka, T., Hocker, L.O., Benedek, G.B.: Spectrum of light scattered from a viscoelastic gel. J. Chem. Phys. **59**, 5151–5159 (1973)
8. Li, Y., Tanaka, T.: Kinetics of swelling and shrinking of gels. J. Chem. Phys. **92**(2), 1365–1371 (1990)

9. Bouklas, N., Huang, R.: Swelling kinetics of polymer gels: comparison of linear and nonlinear theories. Soft Mater. **8**, 8194–8203 (2012)
10. Biot, M.A.: General theory of three-dimensional consolidation. J. Appl. Phys. **12**, 155–164 (1941)
11. Gibbs, J.W.: The scientific papers of J. Willard Gibbs. pp. 184, 201, 215 (1878)
12. Flory, P.J.: Thermodynamics of high polymer solutions. J. Chem. Phys. **10**, 51–61 (1942)
13. Huggins, M.L.: Solutions of long chain compounds. J. Chem. Phys. **9**(5), 440–440 (1941)
14. Flory, P.J., Rehner, J.: Statistical mechanics of cross-linked polymer networks II. Swelling. J. Chem. Phys. **11**, 521–526 (1943)
15. Hong, W., Zhao, X.H., Zhou, J.X., Suo, Z.G.: A theory of coupled diffusion and large deformation in polymeric gels. J. Mech. Phys. Solids **56**, 1779–1793 (2008)
16. Wang, D., Wu, M.S.: Analytical solutions for bilayered spherical hydrogel subjected to constant dilatation. Mech. Mater. **58**, 12–22 (2013)
17. Lai, Y., Hu, Y.H.: Unified solution for poroelastic oscillation indentation on gels for spherical, conical and cylindrical indenters. Soft Matter. **13**, 852–861 (2017)
18. Guo, J.X., Luo, J., Xiao, Z.M.: On the opening profile and near tip fields of an interface crack between a polymeric hydrogel and a rigid substrate. Eng. Fract. Mech. **159**, 155–173 (2016)
19. Treloar, R.G.L.: The Physics of Rubber Elasticity. Oxford University Press, Oxford (1975)
20. Dolbow, J., Fired, E., Ji, H.: Chemically induced swelling of hydrogels. J. Mech. Phys. Solids **52**, 51–84 (2004)
21. Wineman, A., Rajagopal, K.R.: Shear induced redistribution of fluid within a uniformly swollen nonlinear elastic cylinder. Int. J. Eng. Sci. **30**, 1583–1595 (1992)
22. Deng, H., Pence, T.J.: Equilibrium states of mechanically loaded saturated and unsaturated polymer gels. J. Elast. **99**, 39–73 (2010)
23. Deng, H., Pence, T.J.: Shear induced loss of saturation in a fluid infused swollen hyperelastic cylinder. Int. J. Eng. Sci. **48**, 624–646 (2010)
24. Pieper, B., Dulfer, N., Kilian, H.G., Wolff, S.: Thermodynamics of swelling in unfilled and filler-loaded networks. Colloid Polym. Sci. **270**, 29–39 (1992)
25. Chester, S.A., Anand, L.: A coupled theory of fluid permeation and large deformation. J. Mech. Phys. Solid. **58**, 1879–1906 (2010)
26. Drozdov, A.D., Christiansen, J.deC.: Constitutive equations in finite elasticity of swollen elastomers. Int. J. Solid Stuct. **50**, 1494–1504 (2013)
27. Li, B., Chen, H., Li, D.: Effect of solvent diffusion on reactive chromotropic polyelectrolyte gel. Int. J. Appl. Mech. **08**, 4401–4412 (2016)
28. Dai, O., Akifumi, K., Nobutada, O.: Using two scaling exponents to describe the mechanical properties of swollen elastomers. J. Mech. Phys. Solids **90**, 61–76 (2016)
29. Tang, S., Glassman, M.J., Li, S., Socrate, S., Olsen, B.D.: Oxiadatively responsive chain extension to entangle engineered protein hydrogels. Macromolecules **47**, 791–799 (2014)
30. Kaliske, M., Heinrich, G.: An extended tube-model for rubber elasticity: statistical-mechanical theory and finite element implementation. Rubber Chem. Technol. **72**, 602–632 (1999)
31. Meissner, B., Matejka, L.: A Langevin-elasticity-theory-based constitutive equation for rubberlike networks and its comparison with biaxial stress–strain data. Part I. Polymer **44**, 4599–4610 (2003)
32. Miehe, C., Göktepe, S., Lulei, F.: A micro-macro approach to rubber-like materials—Part I: the non-affine micro-sphere model of rubber elasticity. J. Mech. Phys. Solids **52**, 2617–2660 (2004)
33. Kroon, M.: An 8-chain model for rubber-like materials accounting for non-affine chain deformations and topological constraints. J. Elast. **102**(2), 99–116 (2010)
34. Edwards, S.F., Vilgis, T.A.: The effect of entanglements in rubber elasticity. Polymer **27**, 483–492 (1986)
35. Davidson, J.D., Goulbourne, N.: A nonaffine network model for elastomers undergoing finite deformations. J. Mech. Phys. Solids **61**, 1784–1797 (2013)
36. Yan, H.X., Jin, B.: Influernce of microstructural parameters on mechanical behavior of polymer gels. Int. J. Solids Struct. **49**, 436–444 (2012)
37. Yan, H.X., Jin, B., Gao, S.H., Chen, L.W.: Equilibrium swelling and electrochemistry of polyampholytic pH-sensitive hydrogel. Int. J. Solids Struct. **51**, 4149–4156 (2014)
38. Yang, Q.S., Ma, L.H., Shang, J.J.: The chemo-mechanical coupling behavior of hydrogels incorporating entanglements of polymer chains. Int. J. Solids Struct. **50**, 2437–2448 (2013)
39. Rubinstein, M., Panyukov, S.: Elasticity of polymer networks. Macromolecules **35**, 6670–6686 (2002)
40. Arruda, E.M., Boyce, M.C.: A three-dimensional constitutive model for the large stretch behavior of rubber elastic materials. J. Mech. Phys. Solids **41**(2), 389–412 (1993)
41. Li, Y., Tang, S., Kröger, M., Liu, W.K.: Molecular simulation guided constitutive modeling on finite strain viscoelasticity of elastomers. J. Mech. Phys. Solids. **88**, 204–226 (2016)
42. Hong, W., Liu, Z., Suo, Z.G.: Inhomogeneous swelling of a gel in equilibrium with a solvent and mechanical load. Int. J. Solids Struct. **46**, 3282–3289 (2009)
43. Bischoff, J.E., Arruda, E.M., Grosh, K.: A new constitutive model for the compressibility of elastomers at finite deformation. Rubber Chem. Technol. **74**, 541–559 (2001)
44. Gaylord, R.J., Douglas, J.F.: Rubber elasticity: a scaling approach. Polym. Bull. **18**(4), 347–354 (1987)
45. Gaylord, R.J., Douglas, J.F.: The localization model of rubber elasticity II. Polym. Bull. **23**(5), 529–533 (1990)
46. Douglas, J.F.: The localization model of rubber elasticity. Macromol. Symp. **291–292**(1), 230–238 (2010)
47. Douglas, J.F.: Influence of chain structure and swelling on the elasticity of rubber materials: localization model description. Macromol. Symp. **329**(1), 87–100 (2013)
48. During, C.J., Morman, K.N.: Nonlinear swelling of the polymer gels. J. Chem. Phys. **98**, 4275–4293 (1993)
49. Lou, Y., Robisson, A., Cai, S., Suo, Z.: Swellable elastomers under constraint. J. Appl. Phys. **112**, 1059–590 (2012)

50. Chester, S.A., Anand, L.: A thermo-mechanically coupled theory for fluid permeation in elastomeric materials: application to thermally responsive gels. J. Mech. Phys. Solid. **59**, 1978–2006 (2011)
51. Bouklas, N., Landis, C.M., Huang, R.: A nonlinear, transient finite element method for coupled solvent diffusion and large deformation of hydrogels. J. Mech. Phys. Solid. **79**, 21–43 (2015)
52. Cai, S., Suo, Z.: Equations of state for ideal elastomeric gels. Eur. Phys. Lett. **97**, 34009 (2012)
53. Chen, Z., Cohen, C., Escobedo, F.A.: Monte Carlo simulation of the effect of entanglements on the swelling and deformation behavior of end-linked polymeric networks. Macromolecules **35**(8), 3296–3305 (2002)
54. Drozdov, A.D., Christiansen, J.deC.: Stress–strain relations for hydrogels under multiaxial deformation. Int. J. Solids Struct. **50**, 3570–3585 (2013)
55. Bitoh, Y., Akuzawa, N., Urayama, K., Takigawa, T., Kidowaki, M., Ito, K.: Peculiar nonlinear elasticity of polyrotaxane gels with movable cross-links revealed by multiaxial stretching. Macromolecules **44**, 8661–8667 (2011)
56. Zhang, H.: Strain–stress relation in macromolecular microsphere composite hydrogel. Appl. Math. Mech. (English Ed.) **37**, 1539–1550 (2016)